Desalination 378 (2016) 100–107

Contents lists available at ScienceDirect

Desalination

journal homepage: www.elsevier.com/locate/desal

freepaper.me FREE paper

Experimental investigation of a multi-effect isothermal heat with tandem solar desalination system based on humidification–dehumidification processes

Gang Wu [a], Hongfei Zheng [a,*], Huifang Kang [a], Yingjun Yang [a], Peng Cheng [a], Zehui Chang [b]

[a] School of Mechanical Engineering, Beijing Institute of Technology, Beijing 100081, China
[b] College of Energy and Power Engineering, Inner Mongolia University of Technology, Hohhot 010051, China

HIGHLIGHTS

- The sketch of a three-stage multi-effect solar HDH desalination process is given out.
- The maximum PR at the heating temperature of 85 °C can reach about 2.65.
- When the feed water rate is 2 t/h, the maximum yield can reach 182.47 kg.
- The yield per volume is calculated as 22 kg/m^3 h.

ARTICLE INFO

Article history:
Received 29 June 2015
Received in revised form 6 September 2015
Accepted 25 September 2015
Available online 22 October 2015

Keywords:
Solar desalination
Humidification–dehumidification
Isothermal heat
Tandem
Three-stage

ABSTRACT

A new multi-effect solar desalination system based on humidification–and dehumidification (HDH) process was investigated experimentally in this paper. Several hourly yields with operation temperatures were tested and analyzed. The warm saline water is sprayed upon the porous ball humidifiers, which is simple and effective for enhancing the evaporation process. A mathematical model based on the mass and energy balances in each unit of the system is developed which is used to optimize the test. In addition the performance ratio (PR) of the device was investigated under different feeding water mass flow rates and heating temperature conditions. The experimental results indicate that the yield of system increases with the increase in water flow rate and air flow rate. The maximum PR of the system at the heating temperature of 85 °C can reach up to about 2.65. When the heating temperature increases from 60 to 90 °C and the feed water flow rate is 2 t/h, the fresh water yield increases from 59.41 to 182.47 kg/h. The yield per unit volume is calculated as 22 kg/m^3 h. The numerical results based on the mathematical model are well in agreement with the experimental results. The maximum relative deviation is only 5%.

© 2015 Elsevier B.V. All rights reserved.

1. Introduction

Fresh water shortage has become one of the most serious worldwide problems with the continuous increase of world population. Conventional desalination techniques, such as multi-effect distillation (MSF), membrane distillation (MD), reverse osmosis (RO) and electrodialysis require conventional fuels, which are not suitable for the object of sustainable development. Solar desalination processes are recognized as a feasible method to solve the above problems [1].

Nowadays, air humidification–dehumidification (HDH) process has been successfully used for solar desalination, which has some advantages such as simple process, possible to use low temperature heat energy, working under constant pressure, easy installation and low operating cost. It can be used in rural areas to produce fresh water for drinking or irrigation [2–5]. Based on the characteristics mentioned above, solar HDH is being investigated by many researchers.

Solar air HDH system can be generally separated into two main operation modules. One is that the air in the system is heated by solar air collectors to recover the moisture absorption capacity of air. The other is that the seawater in the system is heated by solar water collectors. Then the hot seawater is used to heat and humidify the circulation air to produce the fresh water.

To improve the performance of air-heated systems, Chafik [6] proposed a three-stage cycle system. The system is a modularized one with three independent components — two solar collectors, an evaporator and a condenser. By separating the evaporation and condensation processes and by incorporating regenerative heating of the feed water in the condenser, most of this energy can be recaptured. The idea of this scheme is to increase the air humidity in each stage so that the

* Corresponding author.
E-mail address: hongfeizh@bit.edu.cn (H. Zheng).

http://dx.doi.org/10.1016/j.desal.2015.09.024
0011-9164/© 2015 Elsevier B.V. All rights reserved.

whole water production can be increased. Chafik finally increased the exit moisture capacity up to about 4.5% (by weight) for a single stage system and about 9.3% for a four-stage system.

Amara et al. [7] presented a novel air multiple effect humidification–dehumidification working method and analyzed its main operating parameters. This system was used to simulate a seawater desalination process driven by an eight-stage air solar collector. It was found that the ratio of water to dry air mass flow rates was optimized to be about 45%.

A simple multi-stage HD desalination system (with 3 stages) is given by reference [8]. The hot water from each upper stage humidifier is sent into the low stage humidifier and the outlet of each low stage condenser is linked to the inlet of the upper stage condenser. According to the report, the productivity of the entire system could be increased by 20% when compared with a single stage system. A small pilot plant with four-stage humidification was established by Houcine et al. [9]. The daily freshwater output reached 355 kg under the average intensity of solar radiation of 590 W/m^2.

The research results of the conventional solar desalination shows that although the energy utilization rate will increase with the increase of stage number in HDH system, the fresh water production will not increase obviously. The reason is that when the stage number increases, the average temperature in the system will decrease so that the average air humidity in the system will decline substantially. Finally, the production rate per unit volume will be reduced. Until the 1990s, many researchers focused on how to optimize the operating performance of the humidification and dehumidification process, reuse the rejected water and the latent heat of vaporization in order to gain a high energy recovery rate.

Hou et al. [10] proposed a so called 'pinch technology' to optimize the ratio of seawater to air flow rate (L/G). According to the pinch technology and reusing waste heat of rejected brine water, the gain output ratio (GOR) of the HDH system will be promoted by about 2–3 for 3 stages of basin type [11]. For validation of the pinch technology, Hou [12] established a 2-stage system and obtained about 83.6% energy recovery ratio when the pinch temperature is 1 °C.

Ghalavand et al. [13] studied a new humidification–dehumidification process which was named "Humidification Compression (HC)". A compressor was used to increase the pressure and temperature of the humid air coming from the humidifier and a throttling value was used to reduce the pressure coming from the dehumidifier in a closed-air cycle. The gain output ratio (GOR) which is the ratio of the latent heat of vaporization of the fresh water produced to the total energy input by the compressor was calculated to be 2.07 for one-effect system.

A model and a structured procedure to optimize the shape and structure of a multi-effect humidification–dehumidification desalination system were introduced by Morteza et al. [14]. Based on considering the maximum production rate as the objective function, the optimum design parameters of the multi-effect humidification–dehumidification desalination unit were derived by using the genetic algorithm method under the fixed total volume condition. The results showed that the inlet cold and hot water temperatures and the column heights played important roles in the construct design of a multi-effect humidification–dehumidification desalination unit.

Kang et al. [15] developed a mathematical model to investigate the performance of a two-stage multi-effect desalination system based on the humidification–dehumidification process with the variation of the control parameters. Chang et al. [16] studied the effect of seawater flow rates on the production of a solar desalination plant using porous ball technique and new circulation ways. The research achieved more than 2 of GOR for a two effect system.

In a word, many researchers contributed to solar desalination systems by HDH processes especially in improving the system energy usage efficiency. However, they do not pay enough attention to the production rate per unit volume of the system which is a shortcoming of HDH desalination systems relative to other desalination methods. In traditional solar HDH desalination systems, only parts of the stage work in high temperature. The operation temperature in other stages will decrease step by step with the increasing stage number. On the other hand, all of the seawater entering in the system will be heated to the highest temperature which will waste too much sensible heat energy. To further improve the performance of solar HDH desalination, this paper presented a novel tandem isothermal heating HDH desalination method and a three-stage multi-effect HDH system. Compared with the previous multi-effect HDH systems, this system cannot only reuse the latent heat of condensation and recycle the residual heat in the brine but also most stages can operate in highest temperature except for the lowest stage which can further improve specific volume yield. Moreover, it only needs to heat part of the feed water resulting in saving of energy. The present work assessed the performance of the device under different operation conditions and experimentally validated the mathematical model of the system developed by Kang [15].

2. Description of the experimental set-up and the working principle

2.1. Structure parameters and working principle

The humidification–dehumidification process is based on the fact that the moisture content of air increases progressively with elevated temperature. For instance, 1 kg of dry air can carry almost 1.25 kg vapor or more when its temperature increases from 60 to 90 °C.

The system presented in this paper consists of four closed loops: a solar loop which can produce hot water and three water desalination loops with the function of producing desalinated water. The solar loop is a thermosyphon water heater connected with a heat exchanger to deliver heat to the seawater.

The desalination loops include three evaporation towers with hot seawater sprayers and three condensation towers which are configured to form an upper loop and a lower loop. Air is circulated by fans within each loop. Fig. 1 illustrates a schematic diagram of the experimental set-up and Fig. 2 shows its photograph.

In the condensation sections, the three heat exchangers which are made of copper tubes with corrugated aluminum fins are connected to each other in series. The porous plastic balls are chosen to establish the packed bed. To increase the contact surface between air and seawater, the porous plastic balls were packed in the evaporation sections to achieve a larger wetted surface and an efficient humidification of the air. The shell of evaporators and condensers were constructed of 3 mm stainless steels by welding and were insulated by styrofoam layers with a thickness of 25 mm. The operation principle of this desalination process is presented as follows.

Firstly, the seawater is fed to the low condensation tower (LCT) to condense the moist air coming from the low evaporation tower (LET). The latent heat of condensation is used to preheat the feed water. At the exit of the LCT, a small part of seawater is expelled from the system and the remainder enters the middle condensation tower (MCT) to condense the water vapor in the moist air flowing from the middle evaporation tower (MET). After that, the heated seawater is divided into two parts. One enters the high evaporation tower (HET) through the moisturizing sprayer in HET and the other flows into the LET by the evaporating sprayer. The brine accumulated at the bottom of the HET is circulated through the heat exchanger where the brine is heated up and returned to the HET through evaporating sprayer. In the HET, due to heat and mass transfers between the hot brine and the air stream, the moisture content of air increases. At the bottom of the HET there is a liquid collector where brine is collected as it drains down to the bottom. In the liquid collector, a vertical overflow pipe is set to ensure the seawater level to a desired degree.

In the middle stage, the brine accumulated at the base of the MET is circulated through the condenser in the HCT where the brine is heated up and then reheated in a heat exchanger. Finally, the brine is returned to the MET through evaporating sprayer in MET.

freepaper.me FREE paper

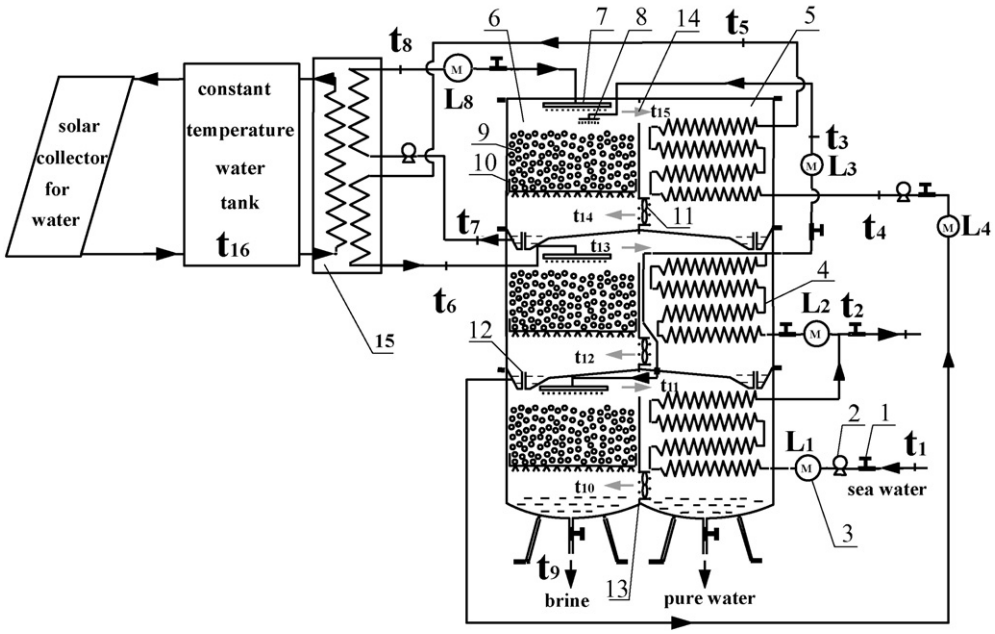

Fig. 1. Schematic drawing of the experimental set-up and the thermocouple locations. 1-value; 2-pump; 3-water flow meter; 4-condenser; 5-dehumidifier; 6-evaporator chamber; 7-evaporating sprayer; 8-moisturizing sprayer; 9-plastic ball; 10-basket; 11-fan; 12-water limited pipe; 13-battle; 14-humid air; 15-heat exchanger; t_1~t_9-Temperature of water at different locations; t_{10}~t_{15}-Temperature of air at air channel; t_{16}-Temperature of water tank.

The novel system operates at atmospheric pressure using air as carrier for vapor. A forced convection heat and mass transfer processes between air and hot brine will occur in the evaporation tower. The forced convection process is assured by an axial flow fan fixed at the bottom of the evaporation tower. The resulted saturated moist air is transported to the condensation tower where it contacts with the condensers and cooled by the seawater to its dew point. Part of the water vapor in the moist air therefore turns into fresh water, which is collected at the bottom of the condensation tower.

Fig. 2. A photograph of the experimental set-up with insulation.

Compared with the previous multi-effect HDH system, the main characteristics of the three-stage multi-effect HDH system are outlined as follows: (1) It cannot only reuse the latent heat of the condensation but also successfully recycles the residual heat in the saline water, so the thermal efficiency of the system could be greatly improved. (2) It has merits of compact structure, stable running, easy control and small floor space occupation. (3) The unit operates under atmospheric pressure with no requirement for pressure-bearing material, so it is of low fee. (4) The unit can operate within a very wide temperature range from 60 °C to 95 °C.

2.2. Size of the experimental unit

The condensation towers have the same structure as the evaporation towers of the unit. The dimension of the single stage distillation chamber is 2.0 × 1.2 × 1.15 m. The air channel, through which the humid air circulates from the humidifier to the dehumidifier, is with the section of dimensions 0.7 m × 0.26 m. Each chamber has one observation window in the wall. The diameter of porous plastic ball is 26 mm, and the thickness of the packed bed is 0.2 m. The capacity of the heating water tank is 250 L. The total area of the heat exchanger is 5 m^2. The maximum seawater flow rate entering low condensation tower by the pump is 3 m^3/h. In addition, feed seawater mass flow rate can be adjusted to a desired value by a valve.

2.3. Data collection

In order to accurately evaluate the performance of the system, a series of indoor experiments for the solar humidification–dehumidification desalination system were carried out. The productivity under steady-state and transient-state condition was investigated. The yield performance under transient-state was examined under a fixed operating temperature. Experimental data include air velocity, circulate seawater temperature, ambient temperature and feed seawater flow rate. The temperatures of the seawater and air at different locations were measured by Pt100 resistance thermometers which are connected to a 32 channel digital logger JLS-XMT. A mercury thermometer, having a minimum scale division of 1 °C, was used to measure the ambient temperature. Feed seawater mass flow rate was measured by using a

freepaper.me FREE paper

Table 1
Technical specifications of instruments used in experimental set-up.

Instrumentation	Range	Accuracy
Average wind speed measurement chip/Kanomax-KA22	0.1–50 m/s	±2%
Liquid turbine flow meter/LWYC-15	0.6–6 m^3/h	±1%
32 channel digital data-recording/JLS-XMT	−200–600 °C	±1%

turbine flow meter which was placed in the seawater circulation loop. The air flow rate was calculated from the air velocity which was measured by a multifunction anemometer with a screw probe at the evaporation tower outlet.

All sensors connected to the data logger were calibrated to determine their sensitivity before starting measurement. During the test period, all the parameters of the transient-state and steady-state experiments were measured and recorded in 5 or 10 min interval respectively. In the steady-state experiment, all parameters keep steady in which the change value of all temperatures in the test points less than 1 °C during 1 h. Each data was recorded three times and the mean value was taken as the test result. The statistical analysis results indicate that the maximum deviation of the yield is less than 8 kg and the maximum relative deviation is less than 5%. The detailed technical specifications of instruments used in the experimental set-up are presented in Table 1.

3. Mathematical modeling

Many researchers have developed the mathematical modeling of the steady-state process of one-stage HDH desalination system [17–20]. For example, Nawayseh in 1999 introduced a classical model based on the mass and energy balances for the evaporator and the condenser as follows.

$$LC_{pw}(t_{Cout}-t_{Cin})+0.5K_{loss}A_{unit}\left(\frac{t_{ta}+t_{ba}}{2}-t_{amb}\right)=G(H_{ta}-H_{ba}) \tag{1}$$

$$LC_{pw}(t_{Cout}-t_{Cin})=K_{cond}A_{cond}\left[\frac{(t_{ta}-t_{Cout})-(t_{ba}-t_{Cin})}{\ln\frac{t_{ta}-t_{Cout}}{t_{ba}-t_{Cin}}}\right] \tag{2}$$

$$LC_{pw}(t_{Hin}-t_{Hout})-0.5K_{loss}A_{unit}\left(\frac{t_{ta}+t_{ba}}{2}-t_{amb}\right)=G(H_{ta}-H_{ba}) \tag{3}$$

$$G(H_{ta}-H_{ba})=KaV\left[\frac{(H_{Hin}-H_{ta})-(H_{Hout}-H_{ba})}{\ln\frac{H_{Hin}-H_{ta}}{H_{Hout}-H_{ba}}}\right] \tag{4}$$

$$Q_{heater}=LC_{pw}(t_{Hin}-t_{Cout}). \tag{5}$$

where C_{in} and C_{out} are the condenser water inlet and outlet, respectively. H_{in} and H_{out} are the humidifier water inlet and outlet, respectively. Subscripts *ta* and *ba* are for air at top and bottom of unit respectively.

We can use their models to calculate our three-stage system. For saving the edition, only the analysis of the mass and energy balances at the high stage was given out. Other two stages may have variety in some details but the process of the heat and mass transfer should be similar.

3.1. High condensation tower

Using the energy balance principle for the HCT unit, the following equations are obtained:

$$L_{c3}C_{pw}(t_5-t_4)+K_{loss}A_3\left(\frac{t_{14}+t_{15}}{2}-t_{amb}\right)=G_3(H_{15}-H_{14}). \tag{6}$$

The right hand side of Eq. (6) describes the reduced energy of the humidified air because of condensing of the humidified air in the HCT. It also indicates the energy supplied to the HCT by the humidified air flow. The first term of the left hand side describes the energy taken away from the HCT by the saline water. The second term of the left hand side describes the energy lost from the wall of the HCT. The system remains stable and the inflow of the energy equals the outflow of the energy as shown in Eq. (6).

The log-mean temperature difference between the humidified air and the saline water is used although the distribution in the condenser is non-linear. The convective heat transfer coefficient K_{cond} is an equivalent parameter. Thus the transferred heat from the humidified air to the saline water through the condenser can be expressed as

$$L_{c3}C_{pw}(t_5-t_4)=K_{cond}A_{cond}\left[\frac{(t_{15}-t_5)-(t_{14}-t_4)}{\ln\frac{t_{15}-t_5}{t_{14}-t_4}}\right]. \tag{7}$$

3.2. High evaporation tower

The spray water in the HET consists of two parts. One part is the hot saline water from the heat exchanger L_8, and the other part is the warm saline water from the HCT L_3. Thus the water mass flow rate in the HET can be obtained as,

$$L_{e3}=L_8+L_3. \tag{8}$$

Applying the previous assumptions the temperature of the spray water on the top of the HET is,

$$t_{e3}=\frac{t_8L_8+t_3L_3}{L_8+L_3}. \tag{9}$$

Similarly, the following equations are obtained,

$$L_{e3}C_{pw}t_{e3}-L_{b3}C_{pw}t_7-L_8C_{pw}t_7 = G_3(H_{15}-H_{14})+K_{loss}A_{unit}\left(\frac{t_{14}+t_{15}}{2}-t_{amb}\right) \tag{10}$$

where

$$L_{b3}=L_3-G_3(W_{15}-W_{14}) \tag{11}$$

where L_{b3} is the brine mass flow rate outlet from the HET, kg/s.

The left hand side of Eq. (10) describes the reduced energy of the saline water in the LET. It also includes the energy supplied to the MET by the saline water flow. Most of the reduced energy is used to vapor the water and then it is taken away by the humidified air flow, as expressed in the first term on the right hand side of Eq. (10). The other is lost in the environment, as expressed in the second term on the right hand side of Eq. (10). The system remains stable, and the inflow of the energy equals the outflow of the energy, as shown in Eq. (10).

freepaper.me FREE paper

Nawayseh et al. [18] derived the following equations for the right hand term of above the

$$G_3(H_{15}-H_{14}) = KaV\left[\frac{(H_{e3}-H_{15})-(H_7-H_{14})}{\ln\frac{H_{e3}-H_{15}}{H_7-H_{14}}}\right]. \quad (12)$$

3.3. Heat source

In the HDD process, the HET outlet water needs to be heated up to the temperature required for the HET entrance. The heat rate needed for heating water with a constant flow rate is given as:

$$Q_{h1} = L_8 C_{pw}(t_8-t_7). \quad (13)$$

Similarly, the MET heat rate needed for heating water with a constant flow rate is given as:

$$Q_{h2} = L_4 C_{pw}(t_6-t_5). \quad (14)$$

The performance of the system can be evaluated by using the above equations.

4. Results and discussion

In the experiment tap water was used instead of seawater. Some electric heaters are installed in the constant temperature water tank to simulate a solar water heater. In addition, the heating power can be adjusted to meet the experimental requirement. The tests were performed to assess the influence of the following parameters on the yield of the system.

1) Water temperature in the thermostatic water tank;
2) Mass flow rate of the circulate seawater;
3) Flow rate of the humid air;
4) Circulate seawater temperature.

4.1. System performance under transient conditions

Transient characteristic is an important indicator for observing system stabilization. Reaching a steady state in a short time is necessary to increase the desalination efficiency of the unit, especially for solar desalination system.

In order to measure the transient characteristic, when the temperature of heating water t_8 reached 60 °C, the unit started to operate and other parameters mentioned above were measured at 5-min interval. Continuous measurements were carried out from 10:00 am to 11:35 am in a day. In addition, the flow rate of the humid air was 2.2 m/s. The 5-min yield and accumulated yield of the unit were recorded. Under the same condition, the temperature of every measured point inside the tower was recorded. The variation curves of the yield with the operation time are shown in Fig. 3, and the temperature variations within 90 min are shown in Fig. 4.

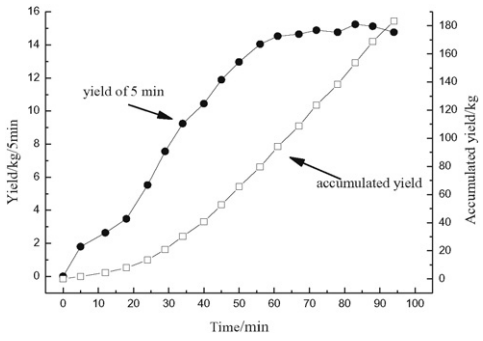

Fig. 3. Variation of the yield in the system with the operation time.

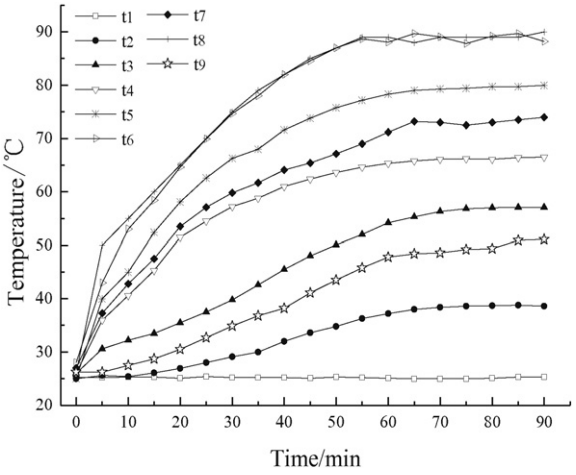

Fig. 4. Variation of the temperature in the system with the operation time.

Fig. 3 shows profiles of the 5-min yield and the accumulated yield variation with the operation time on 16 July 2014. The 5-min yield increased quickly at the beginning of the experiment and reached quasi-steady state at 11:10 am. Meanwhile, the accumulated yield increases with the operation time all the time. The reason of this reaction can be explained by Fig. 4. It can be seen from Fig. 4 that the trend of the variation of the temperature with the operation time at every measured point is the same as that of the 5-min yield. This is due to the increase of the heating temperature causing an increase of the temperature of the moist air entering the dehumidifier. It reveals that the productivity of the system will increase with the increasing relative humidity of the air.

However, the increase of the contact time between the spray seawater and the humid air induces a quickly elevated temperature of the feed seawater, which leads to a less condensation effect and slows the yield growth. After 90 min the quasi-steady state of the system was obtained.

4.2. System performance under steady-state conditions

In the process, the recycled air in the unit undergoes significant changes in heat and mass transfer. Generally, it is difficult to make accurate calculations of the heat and mass transfer in the tower and the yield of the system. In order to simplify the yield calculations the recycled air is considered as saturated at the set temperature. The heat losses from the system are ignored. It is supposed that the pressure inside the unit is 101.3 kPa. The humidity and enthalpy of the saturated air were calculated using the following empirical correlation developed from reported data [18].

$$W = 2.19\times10^{-6}t^3-1.85\times10^{-4}t^2+7.06\times10^{-3}t-0.077 \quad (10)$$

$$H = 0.00585t^3-0.497t^2+19.87t-207.61 \quad (11)$$

where t is the temperature of the saturated air, °C.

Then the fresh water yield of the system produced in the humidifier is

$$G_v = (W_{in}-W_{out})\times v_a \times A \times 3600 \quad (12)$$

where v_a is the humid air flow rate (m/s). A is defined as the effective area of the air channel and A is calculated to 0.18 m^2.

On the basis of ensuring the smooth operation of the process, the test of feed water mass flow rate, heating temperature and humid air flow rate on the unit productivity were studied. Every 10 min, the desired

freepaper.me FREE paper

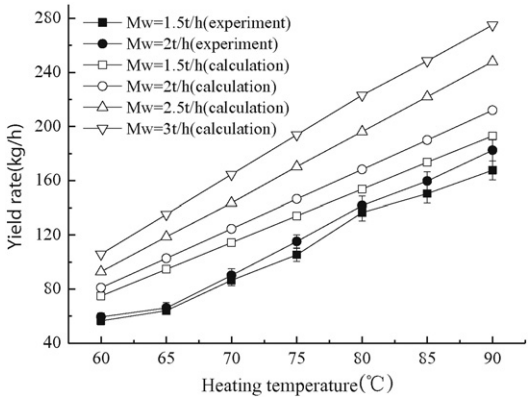

Fig. 5. Variation of the yield with heating temperature in the unit at different water mass flow rates.

parameters were measured and the setting temperatures in the constant temperature water tank were selected as 60 °C, 65 °C, 70 °C, 75 °C, 80 °C, 85 °C and 90 °C separately for half an hour.

Fig. 5 illustrates a comparison between the calculated and the measured variation of the yield with heating at different feed seawater mass flow rates on the device productivity. Limited by time and experiment condition, this paper had tested only the maximum water flow rate at 2 t/h. The vertical bars in the curves are the fluctuations due to the uncertainty of the production rate. For the case studied, the relative deviation of the experimental data is less than 5%. Computer simulation methods are becoming necessary to support the shortage of feed water flow rates. In fact the feed water flow rate of 3 t/h is hard to achieve due to the limitations of the pipe diameter of the condenser. Based on this mathematical model, a steady-state simulation of the yield rate at different water mass flow rates, using Engineering Equation Solver (EES) software [21], has been carried out. It shows that the yield rate increases with an increase of feed water mass flow rate and heating temperature, while the flow rate of the humid air is 2.2 m/s. However, the increase of yield during the heating process varies slowly until the heating temperature reaches 70 °C, after which the trend grows sharply. It can be explained as follows:

(1) Under the same feed water rate, less saline water is evaporated in a packed bed when system operates under low temperature range. So that more of the remaining saline water through the vertical overflows the pipe to the lower humidifier stage. Eventually, more sensible heat along with the overflowed saline water is evacuated to the outside.

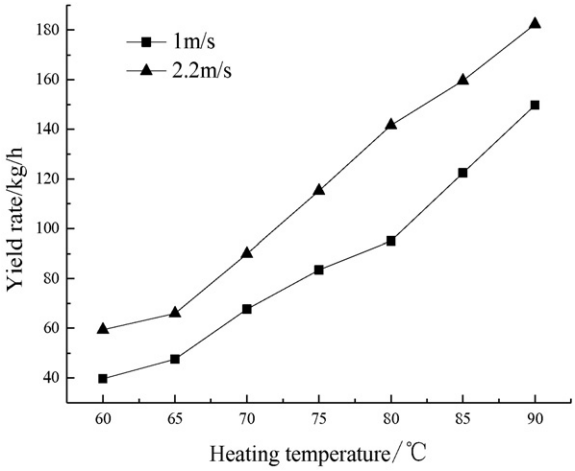

Fig. 7. Effect of air mass flow rate on the system productivity.

(2) The system has some instability. And maybe, it did not reach complete steadiness when we did the test because it will spend more time to reach the steady state when its operation temperature is in low range.

The calculated values of the yield rate agreed well with the experimental results. This also can be explained by Fig. 6. The temperature of the humid air leaving the evaporation tower increases as the heating temperature increased and the temperature difference of the air between the inlet and the outlet of the condensation tower becomes larger along with the increase of relative humidity of the air which leads to more production. Since the condensate temperature is too high in HCT, this will result in low temperature difference between inlet and outlet air ports of the high stage.

Increasing the feed seawater mass flow rate causes a decrease of the temperature of the water leaving the condensers in the LET and HET. The heat transfer between condenser and humid air is strengthened, for the fact that the temperature difference between the feed seawater and the humid air in the condensation tower becomes larger and then induces more yield of the unit.

Fig. 7 shows the effect of the humid air flow rate on the unit productivity. It can be observed in the figure that the yield at the humid air flow rate of 2.2 m/s is more than that at the humid air flow rate of 1 m/s. It reveals that the productivity of the unit will increase with the increasing

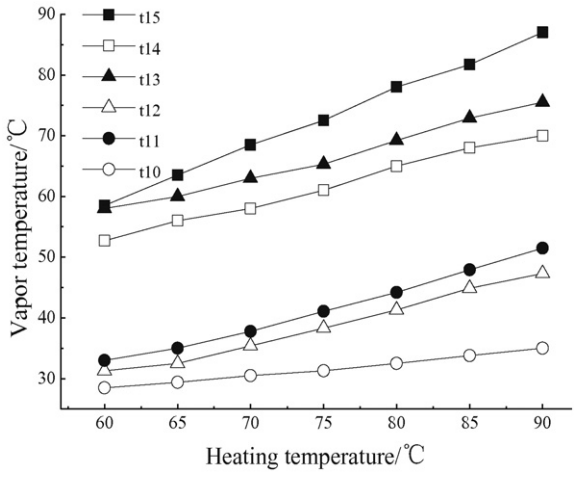

Fig. 6. Variation of the inlet and outlet humid air temperatures with heating temperature.

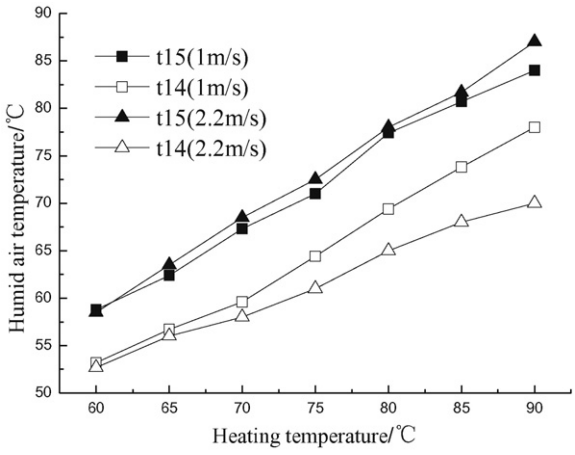

Fig. 8. Effect of air mass flow rate on the humid air temperature.

freepaper.me FREE paper

Table 2
The fresh water yield and the PR of the equipment under steady state.

Heating temperature/°C	$M_w = 1.5$ t/h		$M_w = 2$ t/h	
	Yield/kg	PR	Yield/kg	PR
60	56.50	1.80	59.41	1.87
65	64.11	1.83	66.04	1.92
70	86.58	1.72	90.15	2.12
75	105.41	1.80	115.24	2.20
80	136.51	2.06	141.61	2.33
85	150.34	2.18	159.63	2.65
90	167.62	2.28	182.47	2.58

humid air flow rate because air would carry more water vapor to the condensation tower than before.

This behavior can also be explained by Fig. 8 which shows that when the humid air flow rate increases it causes more water vapor to condense. Since the temperature difference of the humid air at the flow rate of 2.2 m/s is larger than that at the flow rate of 1 m/s, the moisture content of the former leaving the dehumidifier is more. As a result, an increased amount of fresh water can be obtained from the unit.

4.3. Performance of steady-state experiment

Solar desalination system performance basically depends on solar radiation and operation condition. The performance or energy efficiency of humidification–dehumidification desalination system is defined as the performance ratio (PR). A larger value of PR in a desalination system means high energy efficiency and better distillate production performance. Based on the relationship of the input and output energy, the steady-state PR is given as follows:

$$PR = \frac{M_e h_{fg}}{Q_{in} + pt} \tag{13}$$

where M_e is the fresh water production, h_{fg} is the heat of vaporization at the ambient condition, Pt is work of circulating water pump and fan, and Q_{in} is the input energy. In this study, the heat loss of the heaters in the water tank is ignored and the latent heat is calculated at the average partial pressure of water vapor. The total yield and the PR under steady-state are listed in Table 2.

It can be seen from Table 2 that the heating temperature and the feed seawater mass flow rate have significant influence on the unit yield. This result can be explained as follows: the increase of heating temperature increases the temperature of water spraying to the porous plastic balls. Therefore, more moisture content of the humid air leaves the evaporation tower. Consequently, the amount of fresh water obtained from the system is increased. And increasing the feed seawater mass flow rate enlarges the heat transfer temperature difference of the heat exchanger, that is, the effect of condensation heat transfer is strengthened. Increasing the feed seawater mass flow rate also causes a reduction in the moisture content of the air leaving the condensation tower. In the experiment, the PR of the unit can reach to a value between 1.8 and 2.65, indicating that the latent heat of condensation of water vapor can be successfully utilized in the system. Actually, the PR of the unit should increase with the increase of the heating temperature since air would carry more water vapor to condensation tower. However, the PR of the unit does not always increase. In fact, increasing the heating temperature causes an increase in the heat loss. It can be observed from Table 2 that thermal insulation has a significant influence on the PR of the unit especially when the operation temperature is above 85 °C.

5. Conclusions

This paper presents a multi-effect isothermal heat with tandem desalination system based on humidification–dehumidification process and its working principle has been described. Use of porous ball humidifiers enhances the condensation and evaporation process by enlarging the contact surface area. Experimental results show that the system has good transient and steady-state natures. The test results indicate that the system parameters (heating temperature, feed seawater flow rate and humid air flow rate) will influence the process of fresh water production.

Compared with the previous multi-effect humidification–dehumidification desalination system, it not only reuses the latent heat of condensation but also successfully recycles the residual heat in the saline water between the desalination loops. When the heating temperature increases from 60 to 90 °C and the feed water flow rate is 2 t/h, the fresh water yield increases from 59.41 to 182.47 kg/h with the least significant difference of the mean value being $P < 0.05$. The yield per unit volume is calculated as 22 kg/m^3 h and the performance ratio (PR) can reach about 2.65. A numerical model based on the mass and energy balances in each unit of the system is developed and investigated. This novel concept of solar humidification–dehumidification desalination system could be potentially improved for producing more water.

Symbols

A_{cond}	surface area of condenser, m^2
A_3	surface area of HCT, m^2
a	humidifier surface area per unit volume, m^2/m^3
c_{wp}	specific heat of water, J/kg/K
G_3	air mass flow rate in the high stage, kg/s
H	enthalpy, J/kg
K	mass transfer coefficient in humidifier, kg/m^2/s
K_{cond}	overall heat transfer coefficient, W/m^2/K
K_{loss}	heat loss coefficient, W/m^2/K
L	water mass flow rate, kg/s
P	a function of the observed sample results (a statistic) that is used for testing a statistical hypothesis
t	temperature, °C
t_{amb}	ambient temperature, °C
W	saturated humidity, kg_{water}/kg_{dryair}
V	volume of each humidifier, m^3

Subscripts

1	saline water inlet to the LCT
2	saline water outlet from the LCT
3	saline water outlet from the MCT to HET
4	saline water outlet from the MET to HCT
5	saline water outlet from the HCT to heat exchanger
6	saline water outlet from the heat exchanger to MET
7	saline water outlet from the HET to heat exchanger
8	saline water outlet from the heat exchanger to HET
9	saline water outlet from the LET
10	air outlet from the LCT
11	air inlet to the LCT
12	air outlet from the MCT
13	air inlet to the MCT
14	air outlet from the HCT
15	air inlet to the HCT
c3	HCT
e3	HET
b3	brine outlet from the HET

Acknowledgments

This work was supported by the National Natural Science Foundation of China (U1261119), the National Science and Technology Program for rural development during the 12th Five-year plan period

freepaper.me FREE paper

in China (2013AA102407-2), and Natural Science Foundation of Inner Mongolia Autonomous Region, China (No. 2013MS0704) Projects.

References

[1] M. Elimelech, W.A. Phillip, The future of seawater desalination: energy, technology, and the environment, Science 333 (2011) 712–717.
[2] K. Bourouni, M.T. Chaibi, L. Tadrist, Water desalination by humidification and dehumidification of air: state of the art, Desalination 137 (2001) 167–176.
[3] J.A. Miller, V.J.H. Lienhard, Impact of extraction on a humidification–dehumidification desalination system, Desalination 313 (2013) 87–96.
[4] K. Zhani, H.B. Bacha, T. Damak, Modeling and experimental validation of a humidification–dehumidification desalination unit solar part, Energy 36 (2011) 3159–3169.
[5] G.P. Narayan, G. Maximus, S. John, S.M. Zubair, H. John, V. Lienhard, Thermal design of the humidification dehumidification desalination system: an experimental investigation, Desalination 58 (2013) 740–748.
[6] E. Chafik, Design of plants for solar desalination using the multi-stage heating/humidifying technique, Desalination 15 (2004) 55–71.
[7] M.B. Amara, I. Houcine, A. Guizani, M. Maalej, Experimental study of a multiple effect humidification solar desalination technique, Desalination 3 (2004) 209–221.
[8] M. Zamen, S.M. Soufari, S. Abbasian Vahdat, M. Amidpour, M.A. Zeinali, H. Izanloo, H. Aghababaie, Experimental investigation of a two-stage solar humidification–dehumidification desalination process, Desalination 332 (2014) 1–6.
[9] I. Houcine, M. BenAmara, A. Guizani, M. Maalej, Pilot plant testing of a new solar desalination process by a multiple-effect humidification technique, Desalination 5 (2006) 105–124.
[10] S. Hou, D. Zeng, S. Ye, H. Zhang, Exergy analysis of the solar multi-effect humidification–dehumidification desalination process, Desalination 5 (2007) 403–409.
[11] S. Hou, H. Zhang, A hybrid solar desalination process of the multi-effect humidification–dehumidification and basin-type unit, Desalination 220 (1–3) (2008) 552–557.
[12] S. Hou, Two-stage solar multi-effect humidification–dehumidification desalination process plotted from pinch analysis, Desalination 222 (1–3) (2008) 572–578.
[13] Y. Ghalavand, M.S. Hatamipour, A. Rahimi, Humidification compression desalination, Desalination 341 (15) (2014) 120–125.
[14] M. Mehrgoo, M. Amidpour, Derivation of optimal geometry of a multi-effect humidification–dehumidification desalination unit: a constructal design, Desalination 281 (17) (2011) 234–242.
[15] H.F. Kang, Y.J. Yang, Z.H. Chang, H.F. Zheng, Z.C. Duan, Performance of a two-stage multi-effect desalination system based on humidification–dehumidification process, Desalination 344 (2014) 339–349.
[16] Z.H. Chang, H.F. Zheng, Y.J. Yang, Y.H. Su, Z.H. Duan, Experimental investigation of a novel multi-effect solar desalination system based on humidification–dehumidification process, Renew. Energy 69 (2014) 253–259.
[17] N.K. Nawayseh, M.M. Farid, S. Al-Hallaj, A.R. Al-Timimi, Solar desalination based on humidification process: I—evaluating the heat and mass transfer coefficients, Energy Convers. Manag. 40 (13) (1999) 1423–1439.
[18] N.K. Nawayseh, M.M. Farid, A.A. Omar, A. Sabirin, Solar desalination based on humidification process: II—computer simulation, Energy Convers. Manag. 40 (13) (1999) 1441–1461.
[19] A.S. Nafey, H.E.S. Fath, S.O. El-Helaby, A.M. Soliman, Solar desalination using humidification–dehumidification processes. Part II. An experimental investigation, Energy Convers. Manag. 45 (7–8) (2004) 1263–1277.
[20] K. Zhani, Solar desalination based on multiple effect humidification process: thermal performance and experimental validation, Renew. Sust. Energ. Rev. 24 (2013) 406–417.
[21] S.A. Klein, F.L. Alvarado, Engineering equation solver (F-chart software), Middleton, WI, 1993.

freepaper.me FREE paper